

Supporting Information

Enabling Interfacial Compatible and High-Voltage-Tolerant Lithium Metal Batteries with Gradient Compositing Solid- State Electrolytes

Honggang He^a, Jing Shang^a, Shanshan Li^{a,b}, Chunyan Cao^{a,c}, Haifeng Zhang^a, Wei Zhang^{a,*}, Hui Liu^a, Yu Feng^b, Ruiqing Li^a, Shi Chen^d, Bin Fei^{c,*}, Mingzheng Ge^{a,*}

^aSchool of Textile and Clothing, Nantong University, Nantong 226019, P. R. China

^bKey Laboratory of Coal Science and Technology, Ministry of Education, Taiyuan University of Technology, Taiyuan 030024, P. R. China

^cSchool of Fashion and Textiles, The Hong Kong Polytechnic University, Hong Kong 999077, P. R. China

^dInstitute of Applied Physics and Materials Engineering, University of Macau, Macau 999078, P. R. China

*Corresponding authors. E-mail address: zhangwei@ntu.edu.cn (W. Zhang); bin.fei@polyu.edu.hk (B. Fei); mzge1990@ntu.edu.cn (M. Ge)

Supporting information

1. Experimental Section

2. Supporting Figures

Figure S1. SEM images of LLZTO microparticles.

Figure S2. SEM images of LLZTO nanoparticles.

Figure S3. High-resolution XPS spectra of Ta 4f.

Figure S4. The stress-displacement curves of PEO, HLPE and GLPE.

Figure S5. EIS diagram of stainless-steel//stainless-steel symmetric cells using PEO at different temperatures.

Figure S6. EIS diagram of stainless-steel//stainless-steel symmetric cells using HLPE at different temperatures.

Figure S7. EIS diagram of stainless-steel//stainless-steel symmetric cells using HLPE with 1.0828 g LLZTO at different temperatures.

Figure S8. Arrhenius plots of HLPE with 0.1656 g LLZTO and HLPE with 1.0828 g LLZTO.

Figure S9. Long cycling curves of PEO-assembled Li//Li symmetric cells at the current densities of 0.4 mA cm^{-2} .

Figure S10. Long cycling curves of HLPE-assembled Li//Li symmetric cells at the current densities of 0.4 mA cm^{-2} .

Figure S11. SEM images of PEO-assembled symmetric cell after 50th cycles at 60°C and 0.1 mA cm^{-2} current density.

Figure S12. SEM images of HLPE-assembled symmetric cell after 50th cycles at

60 °C and 0.1 mA cm⁻² current density.

Figure S13. SEM images of GLPE-assembled symmetric cell on the GLPE-A side after 50 th cycles at 60 °C and 0.1 mA cm⁻² current density.

Figure S14. SEM images of GLPE-assembled symmetric cell on the GLPE-C side after 50 th cycles at 60 °C and 0.1 mA cm⁻² current density.

1. Experimental section

Preparation of GLPE: $\text{Li}_{6.4}\text{La}_3\text{Zr}_{1.4}\text{Ta}_{0.6}\text{O}_{12}$ (LLZTO) ceramic powders were prepared by the conventional solid-state reaction as described in the previous paper.¹ LLZTO nanoparticles are prepared by dry ball milling of LLZTO microparticles in argon. 0.552 g PEO (polyethylene oxide, $M_w=2,000,000$, Aladdin), 1 g LLZTO microparticles ($\sim 3 \mu\text{m}$) and 0.2 g LiTFSI (bis(trifluoromethane)sulfonimide lithium salt, Aladdin) were dissolved in 12 g ACN (AR, 98%, Aladdin) under vigorously stirring for 24 h. The prepared suspension was poured into a polytetrafluoroethylene dish, and placed in a glove box for 3 h. And then the film was dried in a vacuum oven at 60 °C for 48 h to act as the middle layer. Besides, 0.276 g PEO and 0.1 g LiTFSI were dissolved in 6 g ACN under vigorously stirring for 24 h. The prepared solution was poured into a polytetrafluoroethylene dish and dried in a vacuum oven at 60 °C for 48 hours to work as interfacial repairing layer contacting PEO-rich side, namely PEO electrolyte. Meanwhile, 0.276 g PEO, 0.0828 g LLZTO nanoparticles ($\sim 220 \text{ nm}$), and 0.1 g LiTFSI were dissolved in 6 g ACN under vigorously stirring for 24 h. The prepared solution was poured into a polytetrafluoroethylene dish and dried in a vacuum oven at 60 °C for 48 hours to work as interfacial repairing layer contacting LLZTO-rich side. GLPE with sandwich structure can be achieved by compressing these three layers together under the pressure of 10 MPa and temperature of 60 °C for 1 h.

Preparation of PEO solid electrolyte and HLPE: What's more, 0.552 g PEO, 0.1656 g LLZTO nanoparticles ($\sim 220 \text{ nm}$), and 0.2 g LiTFSI were dissolved in 12 g ACN under vigorously stirring for 24 h. The prepared solution was poured into a polytetrafluoroethylene dish and dried directly in a vacuum oven at 60 °C for 48 hours to obtain HLPE. Similarly, PEO solid electrolyte can be achieved by the same method without adding LLZTO. The thickness of PEO, GLPE and HLPE was controlled at $\sim 150 \mu\text{m}$.

Structure Characterization: The morphology and microstructure were observed by field emission scanning electronic microscopy (SEM, ZEISS, Gemini 300). The chemical valence state and composition of the composites was investigated by XPS

(Thermo Scientific, NEXAS). XRD (Philips) with Cu-K α radiation was used to investigate the crystal structure of the composites. The thermogravimetric analysis (TGA, NETZSCH STA 449 F5) and differential scanning calorimetry (DSC, NETZSCH STA 449 F5) were used to reveal the thermodynamic property of PEO solid electrolyte, HLPE and GLPE, which was performed from 30 to 900 °C at a heating rate of 10 °C min⁻¹. The hardness and modulus were calculated by mechanical tester (MTS C42). The hardness test was conducted in ambient air using nanomechanical test system by using a conical diamond indenter with a 1 μ m tip radius. The maximum load during indentation was 500 μ N.

Electrochemical tests: All cells were assembled in a standard 2025 coin-cell configuration without adding any liquid electrolyte in an Ar-filled glove box. The cathode electrode consists of LiFePO₄ (LFP), poly(vinylidene fluoride) (PVDF) and carbon black with a weight ratio of 8:1:1, which were mixed with N-methyl-2-pyrrolidone and then coated on aluminum foil and dried at 110 °C in a vacuum oven for 12 h. The loading mass of LFP active materials was around 2 mg cm⁻². Cyclic voltammetry (LSV) and electrochemical impedance spectroscopy (EIS) test experiment were tested using an electrochemical workstation (CHI 660E, Chenhua). The SSEs were sandwiched between two stainless-steel (SS) blocking electrodes. The electrochemical impedance spectra were collected at 60 °C with an amplitude of 10 mV within the frequency ranging from 10⁶ to 0.1 Hz. The electrochemical potential window of SSE was examined using a SS as the working electrode and lithium metal as both the reference and counter electrodes by linear sweep voltammetry (LSV) test at a sweep rate of 1.0 mV s⁻¹ from open circuit voltage (OCV) to 6.0 V. The Li transference number (t_{Li^+}) were measured according to the AC impedance and direct-current (DC) polarization (with a polarization voltage of 10 mV) using a symmetric Li//Li cell. All the cells were kept at a temperature of 60 °C for 12 h prior to test. Li//Li symmetric cell were cycled in the galvanostatic mode with a current density of 0.1, 0.2 and 0.4 mA cm⁻² for 1 h at each plating or stripping cycle. The cycling performance and rate capability of Li/GLPE/LFP cells were tested with voltage ranges of 2.8-3.8 V.

2. Supporting figures

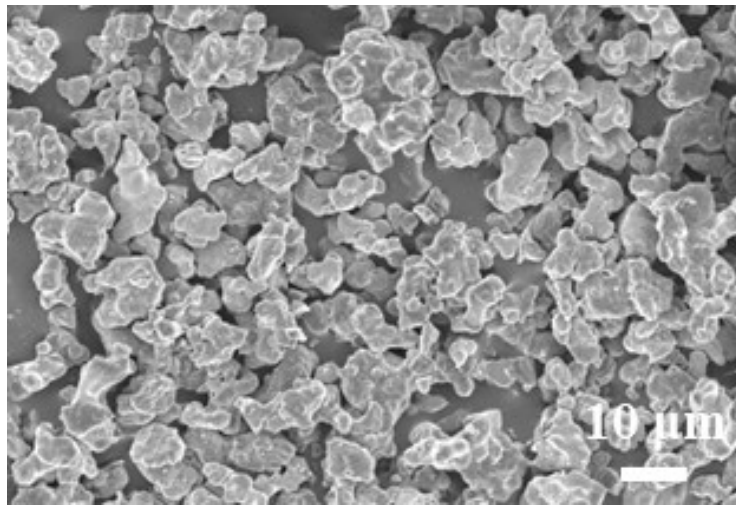


Figure S1. SEM images of LLZTO microparticles.

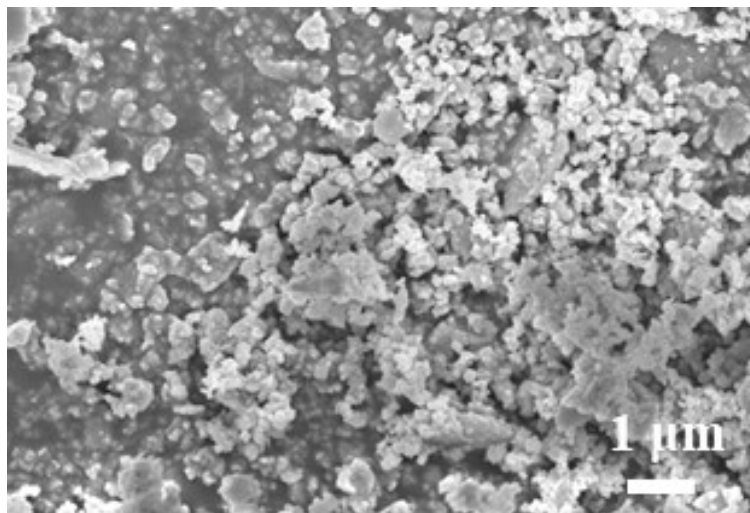


Figure S2. SEM images of LLZTO nanoparticles.

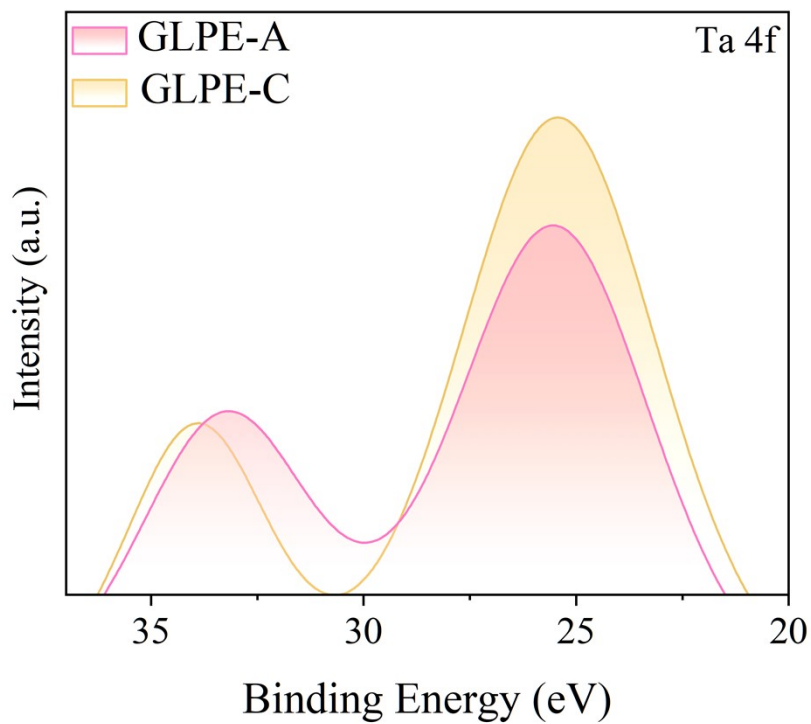


Figure S3. High-resolution XPS spectra of Ta 4f.

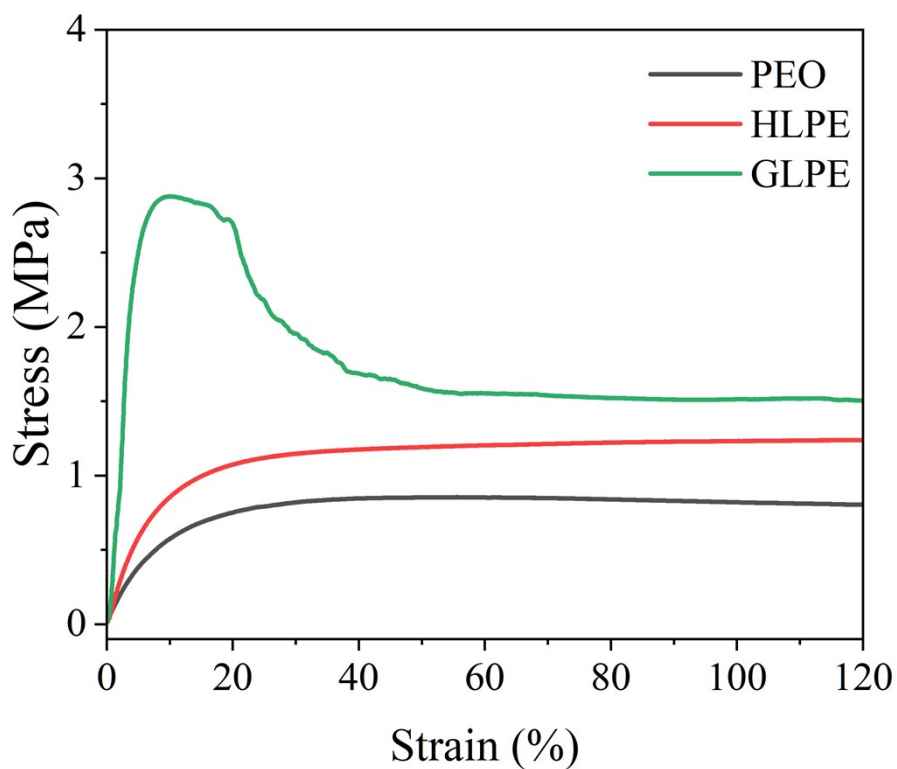


Figure S4. The stress-Strain curves of PEO, HLPE and GLPE.

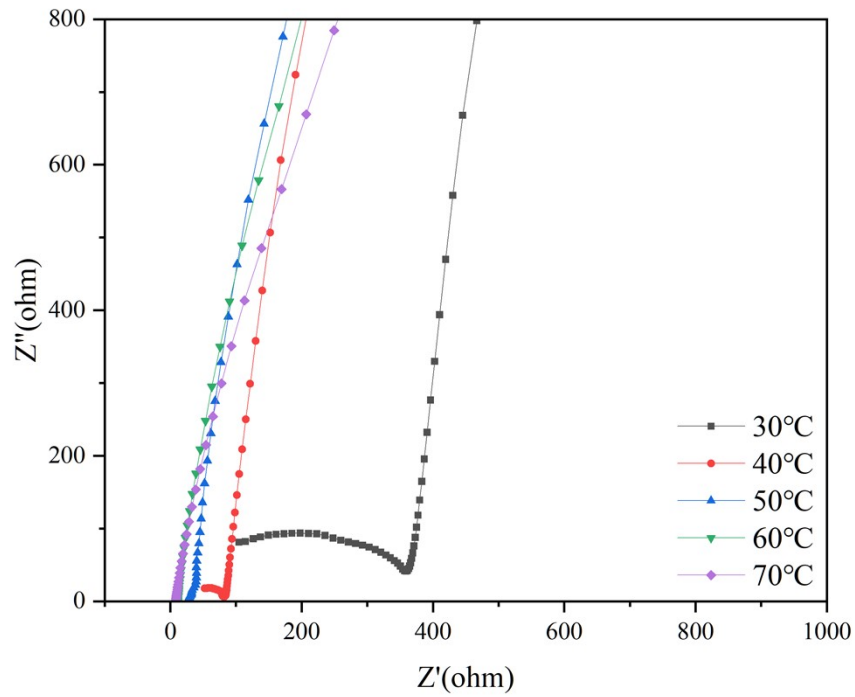


Figure S5. EIS diagram of stainless-steel//stainless-steel symmetric cells using PEO at different temperatures.

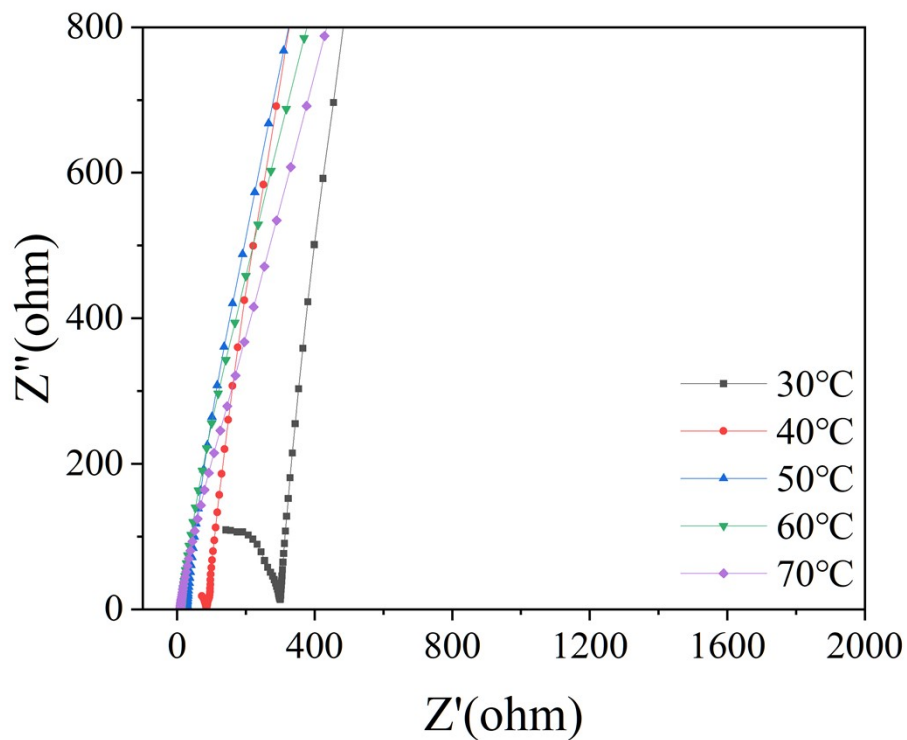


Figure S6. EIS diagram of stainless-steel//stainless-steel symmetric cells using HLPE at different temperatures.

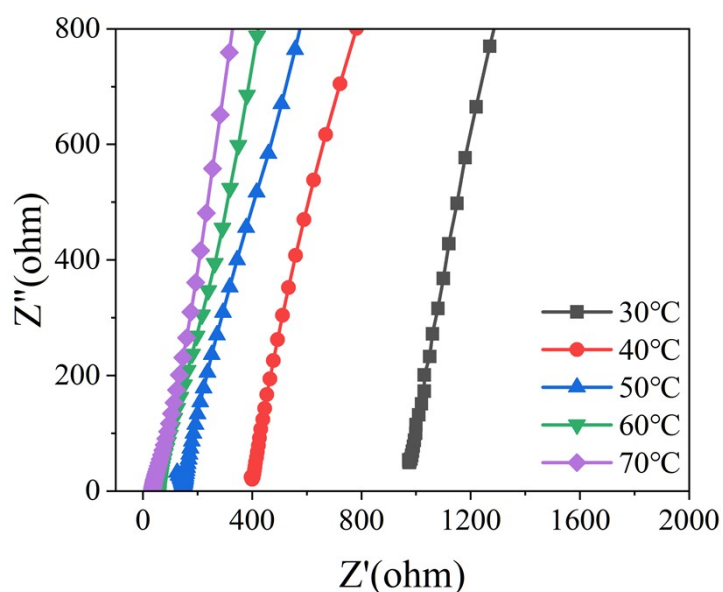


Figure S7. EIS diagram of stainless-steel//stainless-steel symmetric cells using HLPE with 1.0828 g LLZTO at different temperatures.

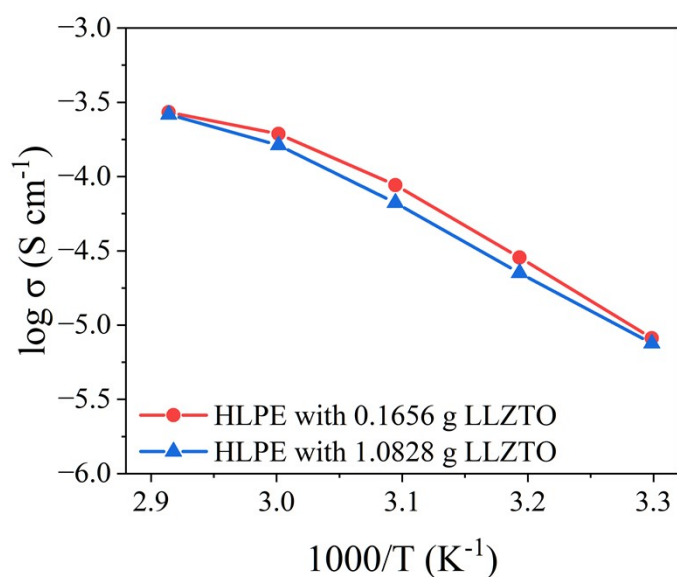


Figure S8. Arrhenius plots of HLPE with 0.1656 g LLZTO and HLPE with 1.0828 g LLZTO.

Discussion: In order to compare the performance of GLPE, the weight of LLZTO particles was increased to 1.0828 g. However, the ionic conductivity ($1.62 \times 10^{-4}\ S\ cm^{-1}$) was lower than that of HLPE with 0.1656 g LLZTO nanoparticles ($1.93 \times 10^{-4}\ S\ cm^{-1}$) due to the aggregation of LLZTO nanoparticles. Meanwhile, the ionic conductivity was much lower than that of GLPE ($3.75 \times 10^{-4}\ S\ cm^{-1}$). Therefore, HLPE with 0.552 g PEO, 0.1656 g LLZTO nanoparticles, 0.2 g LiTFSI, and 12 g ACN was adopted to compare with GLPE.

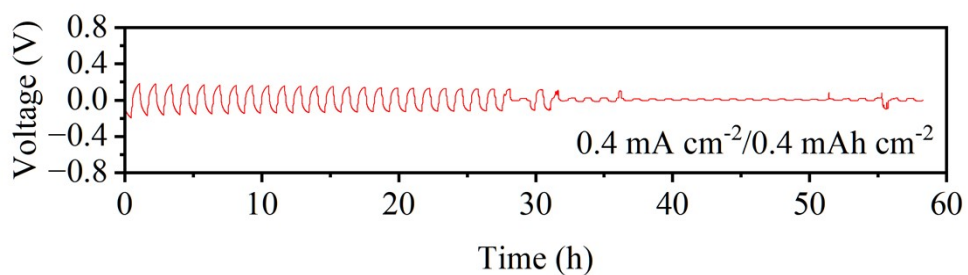


Figure S9. Long cycling curves of PEO-assembled Li//Li symmetric cells at the current densities of 0.4 mA cm^{-2} .

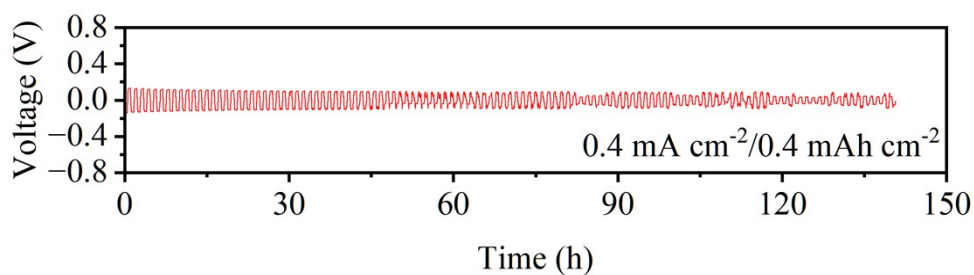


Figure S10. Long cycling curves of HLPE-assembled Li//Li symmetric cells at the current densities of 0.4 mA cm^{-2} .

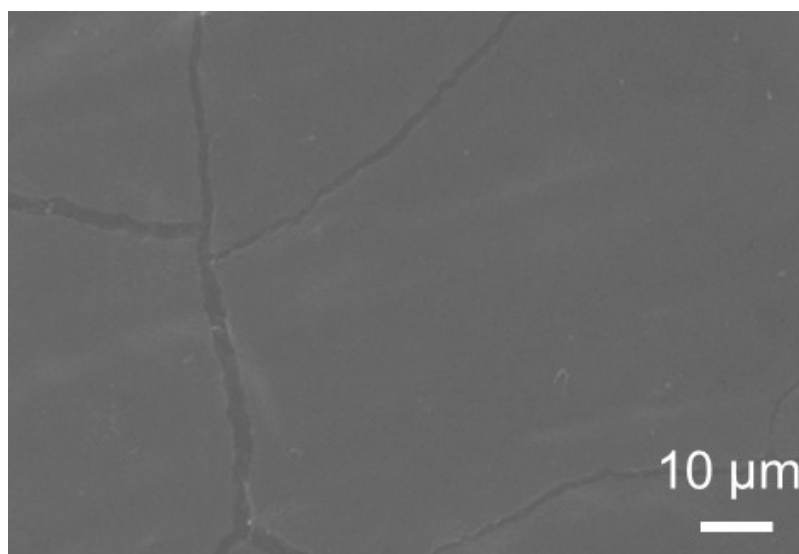


Figure S11. SEM images of PEO-assembled symmetric cell after 50 th cycles at $60 \text{ }^{\circ}\text{C}$ and 0.1 mA cm^{-2} current density.

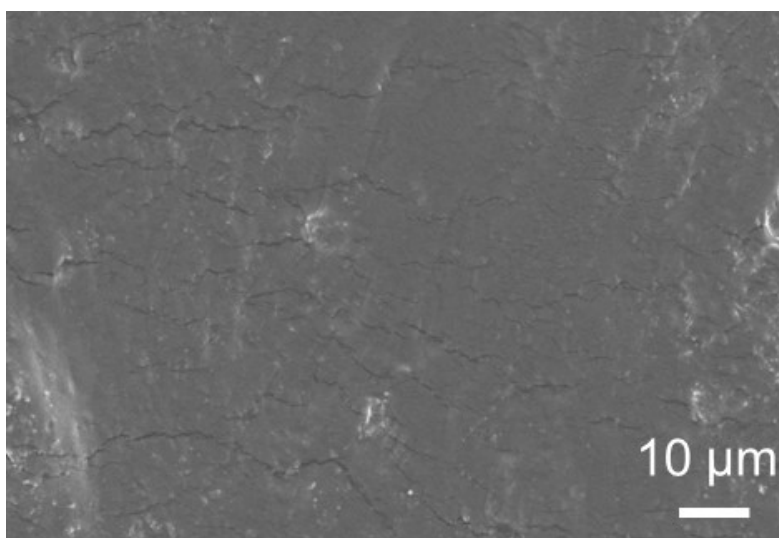


Figure S12. SEM images of HLPE-assembled symmetric cell after 50th cycles at 60 °C and 0.1 mA cm⁻² current density.

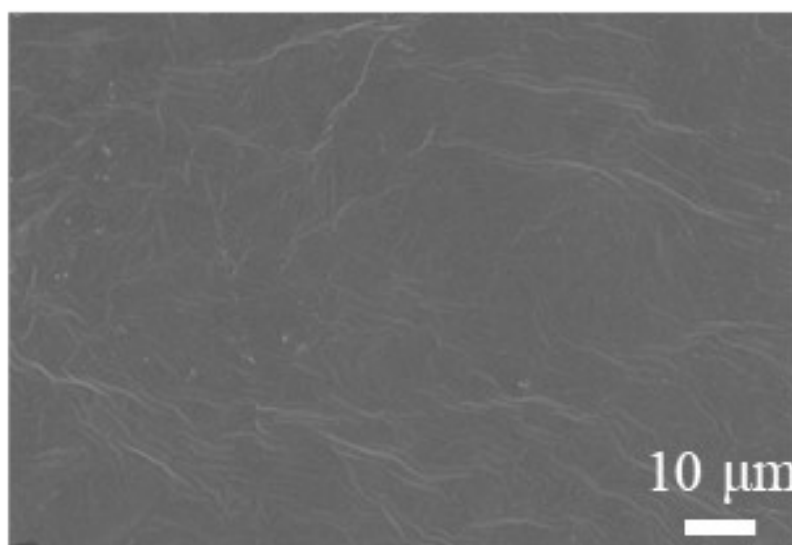


Figure S13. SEM images of GLPE-assembled symmetric cell on the GLPE-A side after 50th cycles at 60 °C and 0.1 mA cm⁻² current density.

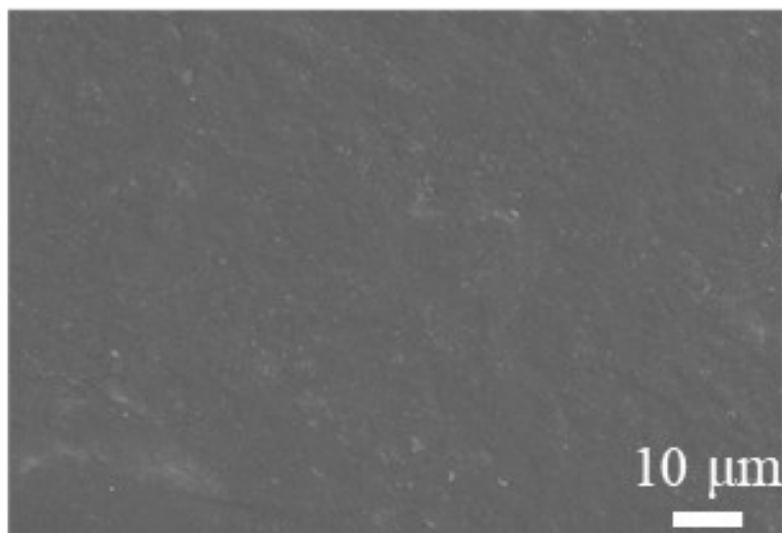


Figure S14. SEM images of GLPE-assembled symmetric cell on the GLPE-C side after 50 th cycles at 60 °C and 0.1 mA cm⁻² current density.

Reference:

(1) Li, Y.; Cao, Y.; Guo, X. Influence of lithium oxide additives on densification and ionic conductivity of garnet-type Li_{6.75}La₃Zr_{1.75}Ta_{0.25}O₁₂ solid electrolytes. *Solid State Ionics*. **2013**, 253, 76-80.